Wave Mixing of Optical Pulses and Bose-Einstein Condensates

Han Pu,[1,2] Weiping Zhang,[1,3] and Pierre Meystre[1]

[1]*Optical Sciences Center, University of Arizona, Tucson, Arizona 85721, USA*
[2]*Department of Physics and Astronomy, Rice University, Houston, Texas 77251, USA*
[3]*Department of Physics, Tsinghua University, Beijing, 100084, People's Republic of China*

(Received 8 May 2003; published 10 October 2003)

We investigate theoretically the four-wave mixing of optical and matter waves resulting from the scattering of a short light pulse off an atomic Bose-Einstein condensate, as recently demonstrated by D. Schneble *et al.* [Science **300**, 475 (2003)]. We show that atomic "pair production" from the condensate results in the generation of both forward- and backward-propagating matter waves. These waves are characterized by different phase-matching conditions, resulting in different angular distributions and temporal evolutions.

DOI: 10.1103/PhysRevLett.91.150407 PACS numbers: 03.75.Kk, 32.80.Qk, 42.50.Ct

The interaction between optical fields and atomic Bose-Einstein condensates has attracted much recent attention, due to its importance in the preparation, manipulation, and detection of condensates, as well as because of its interest in fundamental studies of the nonlinear interaction between Maxwell and Schrödinger waves. A number of phenomena have already been studied both theoretically and experimentally, including matter-wave superradiance [1–3], coherent matter-wave amplification [4–6], and Bragg spectroscopy [7–9].

In a trailblazing experiment [1], a cw laser beam shined on a cigar-shaped condensate resulted in the generation of a fanlike pattern of momentum side modes of the condensate. The initiation of this pattern can be understood in terms of a four-wave mixing process involving two optical fields—the laser field and a so-called end-fire mode; and two matter-wave modes—the condensate and a mode of momentum such that energy-momentum conservation (or phase matching) is satisfied. We recall here that the end-fire mode, first predicted by Dicke [10] in his study of superradiance, corresponds to the privileged direction for spontaneous emission along the long axis of the condensate. Because of momentum conservation, it is clear that the generated side modes must be in the forward direction at a 45° angle between the direction of the incident laser and the long axis of the condensate. The subsequent generation of further side modes results simply from wave mixing involving an already excited side mode instead of the initial condensate at rest.

Recently, that same MIT group [11] reported the results of an experiment where the incident cw laser was replaced by an optical pulse. This led to the remarkable result that for short enough pulses, backward-scattered atoms (with a momentum component antiparallel to the direction of the pump field) were also observed. Moreover, the backward peaks exhibited a slightly different angular distribution compared with the forward peaks. The qualitative difference in diffraction patterns for the short- and long-pulse regimes was attributed to the transition from the Raman-Nath to the Bragg regime of diffraction, that is, to the onset of energy-momentum conservation for long enough interaction times.

In this Letter, we present a theoretical description of this experiment based on an extension of the quasimode approach of Ref. [2]. We give a full dynamical treatment of both the vacuum photon modes and the condensate side modes that interprets the diffraction pattern in terms of atom-photon wave mixing and shows explicitly that the counter-propagating (backward and forward) matter-wave quasimodes result from the quantum-correlated parametric excitation of atomic pairs.

A general theoretical framework to describe the interaction of ultracold atoms with light waves was presented by Zhang and Walls in Ref. [12]. In the situation at hand, the atomic system, assumed to be at zero temperature, interacts with a far off-resonant classical laser field of (real) Rabi frequency Ω_L, wave vector $\mathbf{k}_L$, and frequency $\omega_L = ck_L$, as well as with a continuum of electromagnetic field modes of wave vector $\mathbf{k}$ and polarization λ characterized by the bosonic annihilation operators $B_{\mathbf{k}\lambda}$. In the case of large atom-laser detunings Δ, we are justified in adiabatically eliminating the excited atomic levels, leaving us with just the bosonic ground-state matter-wave field operator $\psi_1(\mathbf{r}, t)$. Under the rotating wave approximation, we find

$$i\hbar\frac{\partial\psi_1}{\partial t} = H_0(\mathbf{r})\psi_1 + \frac{\hbar\Omega_L}{2\Delta}\sum_{\mathbf{k},\lambda}[g^*_{\mathbf{k}\lambda}B^\dagger_{\mathbf{k}\lambda}\times e^{-i(\mathbf{k}-\mathbf{k}_L)\cdot\mathbf{r}-i\omega_L t} + \text{H.c.}]\psi_1, \tag{1}$$

$$i\hbar\frac{\partial B_{\mathbf{k}\lambda}}{\partial t} = \hbar\omega_k B_{\mathbf{k}\lambda} + \frac{\hbar\Omega_L}{2\Delta}g^*_{\mathbf{k}\lambda}e^{-i\omega_L t} \times \int d^3r\, e^{-i(\mathbf{k}-\mathbf{k}_L)\cdot\mathbf{r}}\psi_1^\dagger(\mathbf{r}, t)\psi_1(\mathbf{r}, t), \tag{2}$$

where $g_{\mathbf{k}\lambda} = i\sqrt{2\pi\omega_k/(\hbar V)}\mathbf{d}\cdot\mathbf{e}_{\mathbf{k}\lambda}$ is the coupling strength of the atom with the corresponding vacuum mode (V is the quantization volume, $\mathbf{e}_{\mathbf{k}\lambda}$ the photon

polarization unit vector, and $\mathbf{d}$ the atomic dipole moment). In Eq. (1), the atomic Hamiltonian $H_0(\mathbf{r})$ includes the usual kinetic and trapping potential terms, the ac Stark shift arising from the pump laser, as well as nonlinear atom-atom interactions resulting, e.g., from two-body collisions.

In the absence of electromagnetic fields, the condensate at zero temperature is taken to be in the ground-state $\varphi_0(\mathbf{r})$ of H_0, with $(H_0 - \hbar\mu)\varphi_0(\mathbf{r}) = 0$, μ being the chemical potential. The interaction of this condensate with light shifts the atomic momentum by the photon recoil, and transfers condensate atoms to states of the form $\varphi_0(\mathbf{r})\exp(i\mathbf{q}\cdot\mathbf{r})$. For condensates large compared to an optical wavelength, these states are still approximate eigenstates of H_0, with eigenenergy shifted up by the recoil frequency $\omega_q = \hbar q^2/2M$, an approximation similar to the slowly varying envelope approximation in optics. This suggests expanding $\psi_1(\mathbf{r}, t)$ as [2]

$$\psi_1(\mathbf{r}, t) = e^{-i\mu t}\sum_{\mathbf{q}}\varphi_0(\mathbf{r})e^{i(\mathbf{q}\cdot\mathbf{r}-\omega_q t)}c_{\mathbf{q}}, \tag{3}$$

where the atomic quasimode field operators approximately obey bosonic commutation relations, $[c_{\mathbf{q}}, c^{\dagger}_{\mathbf{q}'}] = \delta_{\mathbf{q},\mathbf{q}'}$. This expansion is valid provided that $q \gg 1/\xi$ where ξ is the healing length of the condensate. Otherwise, it is necessary to account for the collective excitations of the condensate [13]. Inserting then Eq. (3) into Eq. (1) gives

$$i\dot{c}_{\mathbf{q}} = \frac{\Omega_L}{2\Delta}\sum_{\mathbf{k},\lambda}\sum_{\mathbf{q}'}[g^*_{\mathbf{k}\lambda}B^{\dagger}_{\mathbf{k}\lambda}e^{-i\omega_L t}\Pi_{\mathbf{q}-\mathbf{q}'}(\mathbf{k}) + g_{\mathbf{k}\lambda}B_{\mathbf{k}\lambda}e^{i\omega_L t}\Pi^*_{\mathbf{q}'-\mathbf{q}}(\mathbf{k})]e^{i(\omega_q-\omega_{q'})t}c_{\mathbf{q}'}, \tag{4}$$

where $\Pi_{\mathbf{q}}(\mathbf{k}) = \int d^3r\,|\varphi(\mathbf{r})|^2\exp[-i(\mathbf{q}+\mathbf{k}-\mathbf{k}_L)\cdot\mathbf{r}]$ is the spatial Fourier transform of the condensate density profile. Consistently with the slowly varying approximation implicit in the expansion (3), it satisfies the approximate relation $\Pi^*_{\mathbf{q}}(\mathbf{k})\Pi_{\mathbf{q}'}(\mathbf{k}) \approx |\Pi_{\mathbf{q}}(\mathbf{k})|^2\,\delta_{\mathbf{q},\mathbf{q}'}$, a condition that indicates negligible overlap between shifted momentum wave functions.

We now proceed by formally integrating Eq. (2) to find

$$\begin{aligned} B_{\mathbf{k}\lambda}(t) &= B_{\mathbf{k}\lambda}(0)e^{-i\omega_k t} - i\frac{\Omega_L}{2\Delta}g^*_{\mathbf{k}\lambda}e^{-i\omega_L t}\int_0^t d\tau\, e^{-i(\omega_k-\omega_L)\tau}\int d^3r\, e^{-i(\mathbf{k}-\mathbf{k}_L)\cdot\mathbf{r}}\psi^{\dagger}_1(\mathbf{r}, t-\tau)\psi_1(\mathbf{r}, t-\tau) \\ &= B_{\mathbf{k}\lambda}(0)e^{-i\omega_k t} - i\frac{\pi\Omega_L}{\Delta}g^*_{\mathbf{k}\lambda}e^{-i\omega_L t}\sum_{\mathbf{q}_1,\mathbf{q}_2}\Pi_{\mathbf{q}_1-\mathbf{q}_2}(\mathbf{k})\delta(\omega_k - \omega_L + \omega_{q_1} - \omega_{q_2})e^{i(\omega_{q_1}-\omega_{q_2})t}\,c^{\dagger}_{\mathbf{q}_1}(t)c_{\mathbf{q}_2}(t), \end{aligned} \tag{5}$$

where we have used Eq. (3) and have adopted the Markov approximation [14] by replacing $c^{\dagger}_{\mathbf{q}_1}(t-\tau)$ and $c_{\mathbf{q}_2}(t-\tau)$ with $c^{\dagger}_{\mathbf{q}_1}(t)$ and $c_{\mathbf{q}_2}(t)$, respectively, and setting the upper limit of integration over τ to infinity.

It is clear by inspection of Eqs. (4) and (5) that the system dynamics can be interpreted in terms of four-wave mixing processes involving two matter-wave fields (atomic quasimodes $\mathbf{q}$ and $\mathbf{q}'$) and two optical fields (pump laser and a vacuum field mode). Reference [11] interprets the observed pattern as resulting from a sequence of scattering events involving the diffraction of light off a matter-wave grating and the diffraction of atoms off a light grating. Since these two processes occur simultaneously, though, we find our simple four-wave mixing interpretation more appealing. We return to this point and to the relative strengths of both approaches later on.

For optical pulses of short duration, we assume that the condensate population remains undepleted and replace the operators c_0 and $c^{\dagger}_0$ by the c number $\sqrt{N_0}$, where N_0 is the number of condensate atoms. Inserting then Eq. (5) into Eq. (4) results in,

$$\dot{c}_{\mathbf{q}} = \mathcal{A}_{\mathbf{q}}(t)c_{\mathbf{q}} + \mathcal{B}_{\mathbf{q}}(t)c^{\dagger}_{-\mathbf{q}} + \Gamma_{\mathbf{q}}(t), \tag{6}$$

where $\mathbf{q} \neq 0$ and we have only kept the linear terms involving $c_{\mathbf{q}}$ and $c^{\dagger}_{\mathbf{q}}$, consistent with the undepleted pump approximation. We remark that this approximation, which neglects the coupling between subsequent quasimodes, only holds in the initial stage of the wave-mixing process. As such, it cannot describe the fully developed Raman-Nath scattering pattern displayed in Fig. 3 of Ref. [11]. In Eq. (6)

$$\mathcal{A}_{\mathbf{q}}(t) = \frac{N_0\pi\Omega_L^2}{2\Delta^2}\sum_{\mathbf{k},\lambda}|g_{\mathbf{k},\lambda}|^2[|\Pi_{\mathbf{q}}(\mathbf{k})|^2\delta(\omega_k - \omega_L + \omega_q) - |\Pi_{-\mathbf{q}}(\mathbf{k})|^2\delta(\omega_k - \omega_L - \omega_q)],$$

and $\mathcal{B}_{\mathbf{q}}(t) = -\mathcal{A}_{-\mathbf{q}}\exp(2i\omega_q t)$. The Langevin noise operators $\Gamma_{\mathbf{q}}(t)$, which account for the vacuum electromagnetic fluctuations through the initial photon operators and are responsible for the initiation of the scattering process [2], have the form $\Gamma_{\mathbf{q}}(t) = \exp(i\omega_q t)[f^{\dagger}_{\mathbf{q}}(t) - f_{-\mathbf{q}}(t)]$, where

$$f_{\mathbf{q}}(t) = i\frac{\sqrt{N_0}\Omega_L}{2\Delta}\sum_{\mathbf{k},\lambda}g_{\mathbf{k}\lambda}B_{\mathbf{k}\lambda}(0)e^{-i(\omega_k-\omega_L)t}\Pi^*_{\mathbf{q}}(\mathbf{k}).$$

The coefficients $\mathcal{A}_{\mathbf{q}}$ and $\mathcal{B}_{\mathbf{q}}$ each contain two terms, corresponding to the four processes illustrated in Fig. 1. The two processes described by $\mathcal{A}_{\mathbf{q}}$ are resonant, while those described by $\mathcal{B}_{\mathbf{q}}$ are characterized by an energy mismatch $2\hbar\omega_q$, as is evident from the expression for $\mathcal{B}_{\mathbf{q}}$. Figure 1 shows that $\mathcal{B}_{\mathbf{q}}$ describes a pair production process where two condensate atoms are scattered into the quasimodes $\mathbf{q}$ and $-\mathbf{q}$. It is known to result in the production of entangled or squeezed particle pairs. This process, which leads to the generation of

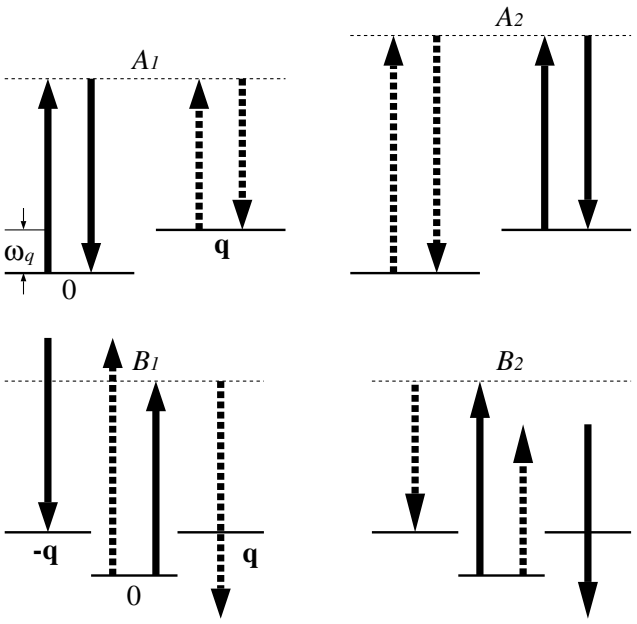

FIG. 1. Plots A_1 and A_2 (B_1 and B_2) are the two scattering processes represented by the coefficient $\mathcal{A}_{\mathbf{q}}$ ($\mathcal{B}_{\mathbf{q}}$). "0" and "$\pm\mathbf{q}$" label the atomic momentum states with 0 being the condensate mode. The solid and dashed arrows represent the pump and scattered photon, respectively.

backward-scattered atoms, occurs for interaction times short enough that energy-momentum conservation (or phase matching) is not yet established. This is why back scattering was not observed in the quasi-cw experiments of Ref. [1], as is also explained in Ref. [11]. Furthermore, $\mathcal{A}_{\mathbf{q}}(t)$ is positive (negative) for forward-(backward-)scattered atoms. Hence, the onset of backward scattering relies fully on the pair production characterized by $\mathcal{B}_{\mathbf{q}}(t)$.

Equation (6) readily gives the quasimode populations $n_{\mathbf{q}} = \langle c_{\mathbf{q}}^{\dagger} c_{\mathbf{q}} \rangle$ as

$$\dot{n}_{\mathbf{q}} = 2\mathcal{A}_{\mathbf{q}} n_{\mathbf{q}} + \mathcal{B}_{\mathbf{q}} m_{\mathbf{q}}^{*} + \mathcal{B}_{\mathbf{q}}^{*} m_{\mathbf{q}} + \mathcal{N}_{\mathbf{q}}, \tag{7}$$

$$\dot{m}_{\mathbf{q}} = (\mathcal{A}_{\mathbf{q}} + \mathcal{A}_{-\mathbf{q}}) m_{\mathbf{q}} + \mathcal{B}_{-\mathbf{q}} n_{\mathbf{q}} + \mathcal{B}_{\mathbf{q}} n_{-\mathbf{q}} + \mathcal{M}_{\mathbf{q}}, \tag{8}$$

where the appearance of the anomalous density $m_{\mathbf{q}} = m_{-\mathbf{q}} = \langle c_{-\mathbf{q}} c_{\mathbf{q}} \rangle$ is a clear signature of the quantum correlations between the modes $\mathbf{q}$ and $-\mathbf{q}$, and the quantities $\mathcal{N}_{\mathbf{q}}$ and $\mathcal{M}_{\mathbf{q}}$ result from the noise operators $\Gamma_{\mathbf{q}}$. Their explicit forms can be obtained using the quantum regression theorem [15] as

$$\mathcal{N}_{\mathbf{q}} = \frac{N_0 \Omega_L^2}{2\Delta^2} \sum_{\mathbf{k},\lambda} |g_{\mathbf{k}\lambda}|^2 |\Pi_{\mathbf{q}}(\mathbf{k})|^2 \, \delta(\omega_k - \omega_L + \omega_q),$$

and $\mathcal{M}_{\mathbf{q}} = -(\mathcal{N}_{\mathbf{q}} + \mathcal{N}_{-\mathbf{q}}) \exp(i2\omega_q t)/2$.

Equations (7) and (8) form a closed set that can be solved numerically. The atomic recoil frequencies ω_q are many orders of magnitude smaller than the laser frequency ω_L, so that conservation of energy requires that the wave numbers of the scattered photons satisfy $k \simeq k_L$. Furthermore, for the large condensates considered here, the slowly varying amplitude approximation mentioned earlier implies that $\Pi_{\mathbf{q}}(\mathbf{k})$ is only significantly different from zero for $\mathbf{k} + \mathbf{q} - \mathbf{k}_L \simeq 0$, indicating momentum conservation for the scattering process. Under such conditions, the atoms are scattered from the condensate in two dipole emission halos, represented schematically by the two circles of radius k_L in Fig. 2.

We evaluate the coefficients in Eqs. (7) and (8) by following Ref. [2] to find $\mathcal{A}_{\mathbf{q}} = \mathcal{B}_{\mathbf{q}} \exp(-i2\omega_q t) = \gamma(\Omega_{\mathbf{q}} - \Omega_{-\mathbf{q}})$, $\mathcal{N}_{\mathbf{q}} = 2\gamma\Omega_{\mathbf{q}}$ and $\mathcal{M}_{\mathbf{q}} = -\gamma \exp \times (i2\omega_q t)(\Omega_{\mathbf{q}} + \Omega_{-\mathbf{q}})$, where $\gamma = N_0 \Omega_L^2 k_L^3 |\mathbf{d}|^2/(4\pi\hbar\Delta^2)$ characterizes the strength of the atom-photon interaction, and $\Omega_{\mathbf{q}} = (4\pi/k_L^2 w^2)[\cos^2\theta_{\mathbf{k}} + (l/w)^2 \sin^2\theta_{\mathbf{k}}]^{-1/2}$. Here, w and l are the dimensions of the cylindrically symmetric condensate along the radial and axial directions, respectively, and $\theta_{\mathbf{k}}$ is the angle between $\mathbf{k}$ ($= \mathbf{k}_L - \mathbf{q}$) and the long axis of the condensate. For a cigar-shaped condensate, $l \gg w$, the scattered photons are predominantly along that axis, Dicke's end-fire mode, so that most of the scattered atoms gain momenta at roughly 45° from the long axis of the condensate [1,2,11].

Figure 3(a) shows the ratio of the backward- and forward-scattered atom numbers along this 45° angle. This ratio is always less than unity in our linear theory [16]. Figure 3(b) shows the angular distribution of the scattered atoms. The forward-scattered atoms form an almost perfect symmetric distribution about the 45° angle. This must be contrasted to the backward-scattered atoms, whose distribution shows an asymmetry, with more atoms scattered into $\phi > 45°$ than into $\phi < 45°$ (see Fig. 2): Backward scattering favors larger angles because the energy mismatch is smaller for $\phi > 45°$ than that for $\phi < 45°$, since $\Delta E = 2\hbar\omega_q \propto \cos^2\phi$. A similar asymmetry in the pattern of scattered atoms was observed experimentally [11], and was attributed to the fact that the two scattering processes occur mainly at different locations along the condensate. While our current theory does not include the atomic and optical [17]

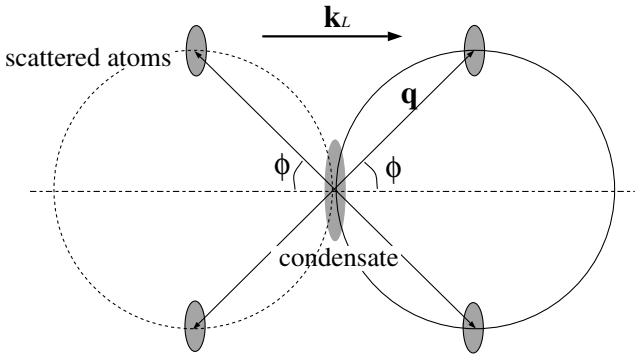

FIG. 2. Schematic of the dipole emission pattern. The circle with solid (dashed) line is traced out by the momenta $\mathbf{q}$ of the forward- (backward-) scattered atoms.

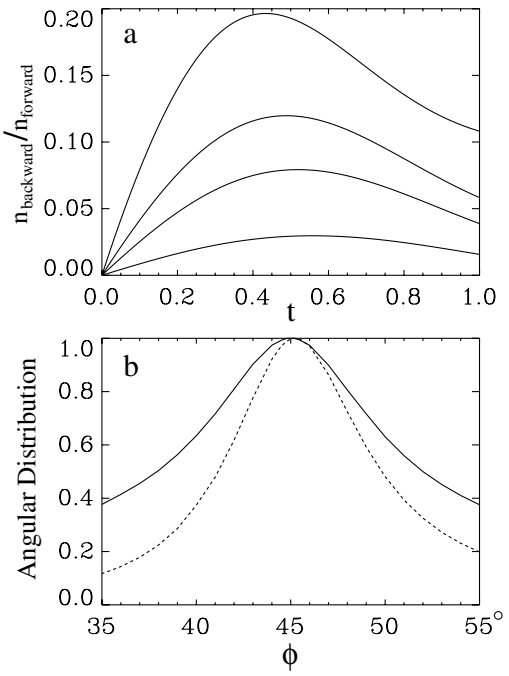

FIG. 3. (a) Ratio of the backward- and forward-scattered atom numbers at angle $\phi = 45°$ as a function of time, in units of $1/\omega_r$, where $\omega_r = \hbar k_L^2/(2M)$. The lines from top to bottom correspond to $\gamma = (500\,250\,150, 50)\omega_r$. (b) Angular distribution in arbitrary units of the forward- (solid line) and backward-scattered (dashed line) atoms. Here $\gamma = 50\omega_r$ and $t = 0.7/\omega_r$. The results are obtained by numerically integrating Eqs. (7) and (8) with initial conditions $n_{\mathbf{q}} = m_{\mathbf{q}} = 0$ using a 4th-order Runge-Kutta method.

multimode propagation effects required to confirm this interpretation, we conjecture that in practice, both phase matching and spatial effects are at play, the former initiating the latter. The two mechanisms could in principle be distinguished by varying the time of flight before detection [18]. This aspect of the problem will be addressed in detail in future work.

In summary, we have presented a theoretical investigation of a zero-temperature condensate interacting with a far off-resonant laser pulse. Our analysis shows that while the resonant Raman scattering illustrated in the plots $A_{1,2}$ of Fig. 1 is the dominant generation mechanism of forward-scattered atoms, the backward-scattered atoms result from the quantum-correlated pair production processes of plots $B_{1,2}$ in Fig. 1 [19]. The lack of phase matching for such pair production processes results in distinct angular distributions for the backward- and forward-scattered atomic peaks, in good qualitative agreement with the experiment of Ref. [11].

The physical picture presented by Schneble *et al.* interprets the backward scattering of the atoms as resulting from Kapitza-Dirac diffraction of matter waves off the optical gratings formed by the pump laser and the end-fire modes [11]. While this point of view is certainly consistent with our correlated pair production picture, we favor the four-wave mixing interpretation, as it clearly demonstrates the interplay of the optical and atomic fields that correlates the backward- and forward-scattered atoms. It also emphasizes that the optical diffraction off the atomic grating and the atomic diffraction off the optical grating are coherently mixed and hence inseparable. For that same reason, the two counterpropagating optical end-fire modes must also exhibit quantum correlations.

In the experiment of Ref. [11], the initial condensate was clearly depleted and higher-order atomic momenta modes were observed. Future work will therefore need to extend our analysis to take the condensate depletion as well as higher-order atomic quasimodes into account. It will also be necessary to describe more carefully the propagation of light through the condensate to gain a full quantitative understanding of this system.

We thank Professor Ketterle for sending us a preprint of Ref. [11] before publication and for discussions. This work is supported in part by the U.S. Office of Naval Research, by the National Science Foundation, by the U.S. Army Research Office, by the NASA Microgravity Fundamental Physics Program, and by the Joint Services Optics Program.

[1] S. Inouye *et al.*, Science **285**, 571 (1999).
[2] M. G. Moore and P. Meystre, Phys. Rev. Lett. **83**, 5202 (1999).
[3] Ö. E. Müstecaplioğlu and L. You, Phys. Rev. A **62**, 063615 (2000).
[4] C. K. Law and N. P. Bigelow, Phys. Rev. A **58**, 4791 (1998).
[5] S. Inouye *et al.*, Nature (London) **402**, 641 (1999).
[6] M. Kozuma *et al.*, Science **286**, 2309 (1999).
[7] J. Stenger *et al.*, Phys. Rev. Lett. **82**, 4569 (1999).
[8] M. Kozuma *et al.*, Phys. Rev. Lett. **82**, 871 (1999).
[9] J. Steinhauer *et al.*, Phys. Rev. Lett. **90**, 060404 (2003).
[10] R. H. Dicke, Phys. Rev. **93**, 99 (1954).
[11] D. Schneble *et al.*, Science **300**, 475 (2003).
[12] W. Zhang and D. F. Walls, Phys. Rev. A **49**, 3799 (1994).
[13] The relevant q's are on the order of the photon wave number, which is a few times $1/\xi$ for the parameters in Ref. [11].
[14] The Markov approximation is justified for the light field inside the Bose-Einstein condensate, since photons escape the condensate in a time short compared to all other times of interest. It is, however, not valid for the atomic quasimodes, see A. Vardi and M. G. Moore, Phys. Rev. Lett. **89**, 090403 (2002).
[15] W. H. Louisell, *Quantum Statistical Properties of Radiation* (Wiley, New York, 1973).
[16] We find numerically that this ratio can approach unity for large γ. However, the undepleted pump approximation is questionable in this limit.
[17] E. Ressayre and A. Tallet, Phys. Rev. A **15**, 2410 (1977).
[18] W. Ketterle (private communication).
[19] Quantum correlations between forward-scattered atoms were previously mentioned by Müstecaplioğlu and You in Ref. [3].